This is a previous version of the article published in Science of The Total Environment. 2017, 577: 183-194. doi:10.1016/j.scitotenv.2016.10.159

Pollutant emissions from the pyrolysis and combustion of viscoelastic memory foam

María A. Garrido, Rafael Font, Juan A. Conesa*

Department of Chemical Engineering, University of Alicante, P.O. Box 99, E-03080 Alicante, Spain

*Email: mangeles.garrido@ua.es

Graphical Abstract

Abstract

Thermal degradation of viscoelastic memory foam (VMF) in a horizontal laboratory scale reactor has been studied. Pyrolysis and combustion experiments under sub-stoichiometric conditions were performed at four different temperatures (550ºC, 650ºC, 750ºC and 850ºC) for the determination of pollutants. Analyses of gas and semivolatile compounds, including polychlorodibenzo-p-dioxins and furans (PCDD/Fs) and dioxin-like polychlorobiphenyls (dl-PCBs) are shown. From the results, it was deduced that pyrolytic conditions favour the formation of PAHs, methane, ethylene, NH_3 and dl-PCBs, whereas the presence of oxygen involves a higher emission of PCDD/Fs and simple N-containing compounds such as NO and HCN. The toxic levels calculated for PAHs, PCDD/Fs and dl-PCBs in all cases were low confirming that the incineration of VMF mattress waste could be a good option for waste management. Nevertheless,

relatively high emissions of NO, NH_3 and HCN were obtained and their reduction must be considered.

Keywords: VMF; NO; HCN; PAHs; PCDD/Fs; dl-PCBs

Abbreviations

B[a]Pe	Carcinogenic potency referred to B[a]P equivalent concentration
ClBzs	Chlorinated benzenes
ClPhs	Chlorinated phenols
dl-PCBs	dioxin-like polychlorobiphenyls
GC-FID	Gas Chromatography-Flame Ionization Detector
GC-MS	Gas Chromatography-Mass Spectrometry Detector
GC-TCD	Gas Chromatography-Thermal Conductivity Detector
HRGC-HRMS	High Resolution Gas Chromatography-High Resolution Mass Spectrometry
HRGC-MS	High Resolution Gas Chromatography-Mass Spectrometry
NCV	Net calorific value
PAHs	Polycyclic Aromatic Hydrocarbons
PCDDs	Polychlorodibenzo-p-dioxins
PCDFs	Polychlorodibenzofurans
VMF	Viscoelastic memory foam

1. Introduction

Viscoelastic memory foam (VMF) is a polyurethane-based foam incorporating additional chemicals to obtain a material that reacts to body heat, allowing the foam to mold to the shape of the body part in contact with it, creating a more uniform pressure distribution which increases the comfort (Shoaib et al., 2014). This temperature-sensitivity is due to the modification of the glass transition temperature of the foam employing chain extender additives (diols with a molecular weight lower than 200, diethylene glycol, 1,4-butanediol, etc.) (Apichatachutapan et al., 2007). VMF is employed to manufacture high quality mattresses and pillows, which can prevent lack of sleep problems. The increase in sleep disorders in the population has meant that the memory foam mattress market has grown 20% in the past eight years and for the next three years, the expected trend is to achieve an annual increase of 7% (Market Research, 2015).

Mattresses waste management presents several problems due to its high volume with an average value of 650 liters per mattress, and consequently in discarded mattresses take up a considerable amount of volume in landfill space. In spite of this fact, landfill is the most usual disposal method for mattress waste, followed by incineration (Hilding, 2014). However, this trend must change in the next few years in order to achieve the targets proposed by the European Parliament for landfilling (European Commission, 2014). These facts, together with the high recoverable energy value of this type of waste, comparable to coal and slightly less than that of fuel oil, make the waste-to-energy the best disposal option (Guo et al., 2014; Nazaré et al., 2012).

VMF was developed in 1966 by NASA's Ames Research Center (Simón et al., 2015), but it did not arrive in the public domain until 1991 when the first viscoelastic mattress was marketed. VMF is a relatively new, material whose thermal decomposition has not been studied and no data regarding volatile and semivolatile compounds have been found. However, several studies about the products generated during the thermal treatment of different types of polymeric wastes have been previously conducted (Font et al., 2011; Garrido et al., 2016b; Guo et al., 2015; Kwon and Castaldi, 2008; Terakado et al., 2014). Reisen et al. (2014) evaluated the volatile organic compounds from the combustion of 10 used building and furnishing materials in a cone calorimeter in order to simulate a well-ventilated fire and the results shown that the highest

55 pollutant concentrations resulted from the combustion of polyester insulation, polystyrene and
56 non-viscoelastic polyurethane foam.
57 Small-scale experimental studies allow the effect of different operational parameters to be
58 evaluated separately and permit boundary conditions for pilot scale or industrial reactors to be
59 established (Couto et al., 2016). In this way, one of the most recent studies was carried out by
60 Zhou et al.(2016) to evaluate the effect of temperature and heating rate on 2-4 ring polycyclic
61 aromatic hydrocarbons (PAHs), gases and HCl formation during the pyrolysis of polyvinyl
62 chloride (PVC) in a laboratory fixed bed reactor. From the results, they concluded that the increase
63 of temperature produced a rise in gases and PAHs yield and a decrease in the HCl formation. A
64 similar effect was observed working at high heating rates.
65 Paraschiv et al.(2015) studied the pyrolysis of five common polymers present in hospital plastic
66 waste in three different fixed bed reactor scales in order to maximize the production of the
67 condensable fraction and optimize its energetic properties. The authors began with the
68 thermogravimetric analysis (TGA) of each polymer and the data obtained in this study were
69 employed to adapt the cooler system of the laboratory reactor to achieve the complete
70 condensation of pyrolysis vapors. Three residence times were employed to perform the small
71 scale experiments, in order to maximize the condensable fraction production. They concluded that
72 the change in the reactor scale did not result in a significant difference in the pyrolysis product
73 distribution.
74 The aim of the present work is to characterize the emissions of pollutants from pyrolysis and
75 combustion of VMF at four different temperatures (550ºC, 650ºC, 750ºC and 850ºC) in a
76 laboratory scale reactor. In this way, the extensive study comprises the analysis of hydrogen,
77 carbon oxides (CO and CO_2), nitric oxide, ammonia, light hydrocarbons, polycyclic aromatic
78 hydrocarbons (PAHs), chlorinated benzenes (ClBzs), chlorinated phenols (ClPhs),
79 polychlorodibenzo-p-dioxins and furans (PCDD/Fs) and dioxin-like polychlorobiphenyls (dl-
80 PCBs), among other semivolatile compounds.
81
82 ## 2. Materials and methods

2.1. Material

The material employed in this study was VMF from a pillow collected from a landfill in Alicante (Spain). The characterization and kinetic study of the pyrolysis and combustion of VMF were recently published (Garrido et al., 2016a). The sample presented a moisture of 1.30% ± 0.04% and an apparent density of 43 kg/m^3, which is the usual value for household and healthcare products (PFA, 2003). The Net Calorific Value (NCV), volatile matter and ash fraction were determined obtaining values of 27.13 ± 1.18 MJ/kg, 99.73% ± 0.10% and 0.11% ± 0.01%, respectively. The elemental analysis showed a content of C, N, H, S and O equal to 61.26% ± 0.16%, 3.34% ± 0.02%, 8.45% ± 0.01%, 0.16% ± 0.16%, and 26.68% ± 0.02%. The foam was apparently not contaminated and due to the homogeneity of the foams, pieces of foam were employed to perform the experiments and previous homogenization was not necessary.

In order to evaluate the possible formation of chlorinated semivolatile compounds such as ClPhs, ClBzs, PCDD/Fs and dl-PCBs, the Cl^- content was analyzed in triplicate following the US EPA 5050 (US EPA, 2007a) and US EPA 9056(US EPA, 2000) methods , where the analysis was performed by ion chromatography (Dionex DX-500, Thermo Fisher Scientific). The Cl^- content was 117 ± 4 mg/kg sample whereas Br^- was not detected.

2.2. Experiments in furnace

The pyrolysis and combustion experiments were performed in a horizontal quartz tubular reactor situated inside a laboratory scale furnace consisting of two different heating zones which was uniformly heated up to the desired temperatures (550ºC, 650ºC, 750ºC and 850ºC). This reactor has been described previously (Aracil et al., 2005; Moltó et al., 2010). In order to achieve the pyrolysis conditions, 350 mL/min (1 atm, 20ºC) of nitrogen (purity of 99.9992%, Carburos Metalicos, Barcelona, Spain) were introduced parallel to the sample, whereas for the combustion experiments synthetic air was employed (purity of 99.995% Carburos Metalicos, Barcelona, Spain) with the same flow rate. The residence times of the gas along the reactor zone at nominal temperatures were calculated considering the different temperature profiles (Aracil et al., 2005) and the values obtained were 4.5 s at 550ºC, 3.8 s at 650ºC, 3.4 s at 750ºC and 3.0 s at 850ºC.

These temperatures were selected bearing in mind the results from the kinetic study developed previously (Garrido et al., 2016a), where it was shown that VMF starts to decompose, independently of the atmosphere employed at around 270ºC and finishes at around 530ºC. At 550ºC, 650ºC and 750ºC decomposition process has finished both in pyrolysis and combustion and these three temperatures are in the range of the typical flexible polyurethane mattress fire temperatures (600-800ºC) (Consumer Product Safety Commision, 2006). Finally, 850ºC was selected because the EU incineration directive establishes 850ºC as the minimum value which should be maintained for at least two seconds in the post-combustion zone (European Communities, 2000).

When the furnace reached the nominal temperature, a 180 mg piece of VMF was placed in a crucible which was introduced into the reactor with a constant speed of 0.21 mm/s. When the sample finished entering the reactor, it was maintained for 4.5 min in order to ensure a correct analysis. The gases evolved from the decomposition of the VMF passed through a packing of quartz rings situated at the end of the reactor which avoided gas bypass and favored further reactions between the primary decomposition gases (Aracil et al., 2005).

The amount of sample and the speed were selected in order to ensure that the combustion experiments were performed under sub-stoichiometric conditions in order to determine the pollutants evolved. Specifically, the oxygen ratio λ, defined as the ratio between the actual oxygen flow and the stoichiometric oxygen flow (Aracil et al., 2010; Font et al., 2010) was around 0.8 (the oxygen available was 80% of the necessary oxygen for complete combustion).

In order to avoid the interference between samples, before each experiment, the reactor was cleaned and heated until 1000ºC in a synthetic air atmosphere. This temperature was maintained for 30 min before using the reactor for the next experiment. In the same way, before the pyrolysis experiments, the reactor was purged with nitrogen for 30 min; enough time to eliminate oxygen considering that the total volume of the reactor is around 150 cm^3.

Four different experiments were performed under pyrolytic and combustion conditions (550ºC, 650ºC, 750ºC and 850ºC); all of them were preceded by the corresponding four blank runs with

137 the reactor without introducing the sample in the crucible. Furthermore, in order to evaluate the
138 reproducibility of the results, the combustion experiment at 850ºC was carried out in duplicate.

139 ## 2.3. Collection of samples and analysis

140 Four series of seventeen experiments (including the blanks) were carried out to collect the
141 different compounds.

142 *2.3.1. Gases and volatile compounds*

143 The first round of experiments was carried out to analyze the gases and volatile compounds
144 (with a boiling point lower than 130ºC), which were collected in 5 L Tedlar® bags at the outlet of
145 the reactor for 14 min. Hydrogen (H_2), carbon monoxide (CO) and carbon dioxide (CO_2) were
146 analyzed by Gas Chromatography coupled to a Thermal Conductivity Detector (GC-TCD,
147 Agilent 7820A GC) using two packed columns (Haye Sep Q 80/100 and Molecular Sieve 5A
148 80/100) coupled with a pneumatic valve. The analysis of aliphatic hydrocarbons (C_1-C_6) together
149 with BTX (Benzene-Toluene-Xylenes) was performed in a Gas Chromatographer with a Flame
150 Ionization Detector (GC-FID, Shimadzu GC-17A) employing an Alumina KCl Plot capillary
151 column. An external standard calibration was employed to detect and quantify each compound.

152 Apart from aliphatic hydrocarbons and BTX, other compounds were detected employing a
153 High Resolution Gas Chromatographer (HRGC) Agilent 6890N with a capillary column DB-624
154 (30 m x 0.25 mm x 1.40 µm, Agilent) and coupled to an Agilent 5973N Mass Spectrometer
155 Detector (MS), working in SCAN mode. An external calibration was also performed employing
156 EPA 502/524.2 VOC Mix (Supelco) as the standard solution.

157 The nitric oxide was analyzed with a portable gas analyzer (IM 2800-P GmbH) also using
158 Tedlar® bags.

159 To analyze the ammonia content in the exhaust gases, an adapted U.S. EPA CTM 027 method
160 was carried out (US EPA, 1997). With this method, ammonia is trapped by an H_2SO_4 0.1 N
161 solution (purity of H_2SO_4 used was 95% (AnalaR NORMAPUR)) as ammonium ion (NH_4^+). For
162 this, the exhaust gases were passed through two impingers containing 50 mL of H_2SO_4 0.1 N
163 solution each one and the solutions were analyzed by Ion Chromatography (Dionex DX5OO).
164

165 *2.3.2. PAHs, ClBzs, ClPhs and other semivolatile compounds*

166 The seventeen experiments were repeated to absorb the semivolatile compounds in a polymeric
167 absorbent (Amberlite XAD-2 resin, Supelco) contained in a tube situated at the outlet of the
168 reactor. Before the solid-liquid extraction, the resin was spiked with three different internal
169 standards in order to quantify semivolatile compounds: 5 μL of deuterated PAHs Mix 26 (Dr.
170 Ehrenstorfer-Schäfers), 10 μL of ^{13}C-labelled ClPhs and 10 μL ^{13}C-labelled ClBzs (Wellington
171 Laboratories). Later, the extraction was performed following the U.S. EPA method 3545A
172 (US EPA, 2007) in an accelerated solvent extraction system (ASE-100 Dionex-Thermo Fisher
173 Scientific) with 50 mL dichloromethane/acetone (1:1 vol.). The extracts were subsequently
174 evaporated with a rotary evaporator and a stream of nitrogen up to a final volume of 1.5 mL and
175 later 3 μL of recovery standard (Anthracene-d10, AccuStandard) were added. The analysis of the
176 semivolatile compounds was performed in an HRGC-MS (Agilent GC 6890N/Agilent MS
177 5973N) following the U.S. EPA 8270D (US EPA, 2014) method as reference. A capillary column
178 HP-5 MS (30 m x 0.25 mm x 0.25 μm, Agilent) was employed for the analysis of PAHs and
179 ClBzs, whereas for ClPhs a capillary column ZB-5MSi (30 m x 0.25 mm x 0.25 μm, Zebron) was
180 used.

181 The detection and quantification of the 16 priority PAHs (US EPA, 1998), from the analysis in
182 SCAN mode, were performed with a standard of each compound by calibration comparing the
183 retention time of the primary ion. Other semivolatile compounds were identified by the
184 comparison mass spectrum of each compound with those of the NIST database, which presented
185 an accuracy higher than 80%; for the quantification, linear interpolations between the response
186 factor (Area/mass) of the two nearest deuterated standards were employed.

187 Both Chlorobenzenes (ClBzs) and Chlorophenols (ClPhs) were analyzed in the SIR mode and
188 the identification of each isomer was performed comparing the primary/secondary ion area ratio
189 with that obtained in the calibration with the labelled compounds

190 *2.3.3. PCDD/Fs and dl-PCBs*

191 The amount of chlorine found in the sample was relatively low (117 mg/kg) although high
192 enough to produce significant amounts of PCDD/Fs and PCBs at levels of ng/kg. In order to
193 increase the possibility of detecting these types of compounds, the gases evolved from six runs in
194 the same conditions (atmosphere and temperature) were absorbed in the same XAD-2 resin tube.
195 In this way, the total mass of sample employed for the analysis of PCDD/Fs and PCBs was around
196 1 g.

197 Resins were spiked with ^{13}C-labeled internal standards of PCDD/Fs and dl-PCBs (10 μL of
198 LCS-1613 for PCDD/Fs and 10 μL WP-LCS diluted to 200 ppm for PCBs, Wellington
199 Laboratories,) and extracted with 50 mL of toluene employing the ASE-100 system. After
200 extraction, the samples were concentrated to change the solvent to hexane. The purification and
201 fractionation of the samples were performed in an automated Power Prep® system (FMS, Inc.)
202 equipped with silica, alumina and activated carbon columns allowing the target compounds to be
203 isolated in two different fractions that were concentrated in a rotary evaporator followed by a
204 gentle stream of nitrogen up to 100 μL and the corresponding recovery standards were added (10
205 μL of ISS-1613 for PCDD/Fs and 10 μL WP-ISS diluted to 200 ppm for PCBs, Wellington
206 Laboratories). The analysis of the samples was performed by HRGC-HRMS on a Micromass
207 Autospec-Ultima NT Mass Spectrometer coupled to an Agilent HP6890 Gas Chromatographer
208 with an Agilent DB-5MS column (60 m x0.25 mm x 0.25 μm) in PTV injection.

209 The analysis of PCDD/Fs was performed by the isotope dilution method employing the relative
210 response factor for each congener obtained previously from calibration standards. The recoveries
211 of the ^{13}C-labeled internal standard PCDD/Fs accomplished the requirements proposed by the
212 EPA 1613 (US EPA, 1994b) method for PCDD/Fs and the EPA 1668C (US EPA, 2010) method
213 for dl-PCBs.

214 In order to summarize the experiments, the number of experiments performed for the different
215 analyses is shown in **Table 1**, where Pyro makes reference to pyrolysis and Comb. to combustion.

216 **Table 1.** Summary of the experiments.

		Analysis							
		Gases and Volatiles		NH_3		Semivolatiles		PCDD/Fs + dl-PCBs	
		Experiments	Runs	Experiments	Runs	Experiments	Runs	Experiments	Runs
Samples	**Blank Pyro.**	4	1	4	1	4	1	4	6
	Pyro.	4	1	4	1	4	1	4	6
	Blank Comb.	4	1	4	1	4	1	4	6
	Comb.	5	1	5	1	5	1	5	6
Total runs		*17*		*17*		*17*		*102*	
Total samples analysed		*17*		*17*		*17*		*17*	

Experiments: Number of temperatures (550, 650, 750 and 850ºC) analyzed. In combustion samples, the analysis at 850ºC was performed in duplicated.
Runs: Number of runs performed under the same conditions (atmosphere and temperature) for each experiment, i.e. in PCDD/Fs+dl-PCBs analysis, the exhaust gases from 6 runs in the same conditions (atmosphere and temperature) was collected in the same XAD-2 resin.

3. Results and discussion

The experimental results are presented in the following Tables and Figures. For the duplicate combustion runs at 850ºC, the standard deviations can also be observed. The two values obtained in the combustion experiments at 850ºC can be found in the Supporting Information.

3.1.Gases and volatile compounds.

The main gases and volatile compounds detected are shown in **Table 2** where letters P and C make reference to Pyrolysis and Combustion experiments, respectively and the numbers accompanying them refer to the different temperatures studied in ºC. Blank runs performed before each experiment presented values lower than 10 ppm, which is the limit of detection calculated (LOD) for these types of compounds. In the same way, compounds with a detected value lower than 10 ppm have been considered as non-detected "nd". The standard deviations calculated from the two combustion experiments at 850ºC represented less than 15% of the average value.

Table 2. Gases and volatile compounds (ppm) detected from the pyrolysis (P) and combustion (C) of VMF at four different temperatures. The average value and standard deviation calculated from two combustion experiments at 850ºC are also shown.

COMPOUND	ppm (μg/g sample)								
	P 550	**P 650**	**P 750**	**P 850**	**C 550**	**C 650**	**C 750**	**C 850**	**σ**

Gaseous compounds										
H_2	521	1753	2897	7383	nd	nd	nd	nd		
CO_2	5826	32058	38595	102099	1241035	1379824	1632718	1919688	±	36659
CO	3000	39297	55554	81358	248356	367658	425903	245279	±	2088
NO	416	341	269	133	505	611	828	1079	±	14
NH_3	321	416	3238	7318	686	1097	1684	2142	±	80
R_{CO}=CO/(CO+CO_2)	0.34	0.55	0.59	0.44	0.17	0.21	0.21	0.11		
Light hydrocarbon compounds										
Analysis by GC-FID										
methane	10344	122750	68738	76546	9387	20273	19784	22201	±	495
ethane	5410	46186	11661	5319	1759	4165	2709	1225	±	72
ethylene	23007	131358	73474	91236	21336	37467	31705	29421	±	326
propane	1854	7774	1097	252	345	690	318	47	±	5
propylene	159	483	106	48	39	55	26	nd		
isobutane	97	249	26	nd	17	28	18	3287	±	100
acetylene	30	442	678	4040	956	1538	1982	110	±	8
n-butane	178	610	470	221	56	123	127	nd		
1-butene	nd	35	nd	nd	nd	nd	nd	nd		
trans-2-butene	nd	nd	nd	nd	80	480	212	nd		
isobutene	234	1402	262	65	19	104	54	nd		
cis-2-butene	83	652	95	29	nd	43	24	nd		
isopentane	69	nd	nd	nd	nd	nd	nd	nd		
n-pentane	nd	132	nd	nd	nd	nd	nd	nd		
propyne	28	62	nd	nd	66	84	86	216	±	5
1,3-butadiene	280	4082	3728	3153	nd	nd	nd	nd		
2-butyne	nd	nd	38	296	nd	nd	nd	nd		
1-butyne	nd	nd	nd	nd	20	27	71	nd		
n-hexane	nd	1422	1117	nd	41	106	258	479	±	10
cis-2-hexene	580	97	40	nd	57	58	31	nd		
benzene	nd	nd	nd	16	nd	nd	nd	nd		
toluene	nd	nd	13	19	nd	nd	nd	nd		
xylenes (m-, p-, o-)	14	14	26	20	nd	11	11	nd		
Analysis by GC-MS										
1-Propene, 2-methyl-	3928	37975	4027	4399	1468	1678	209	nd		
Hydrogen cyanide	nd	3685	5930	9418	3615	5615	9046	17940	±	1239
Acetaldehyde	76374	306389	15782	nd	33168	36198	21147	nd		
1-Buten-3-yne	nd	nd	3009	3401	nd	nd	4372	4056	±	351
Methyl Alcohol	2751	nd	nd	nd	nd	nd	nd	2342	±	235
2-Pentene	nd	20530	4291	2482	6383	8083	4926	nd		
Butane, 2-methyl-	2882	nd	nd	nd	nd	nd	nd	nd		
Cyclopropane, ethyl-	nd	nd	nd	nd	1351	nd	nd	nd		
Cyclopropane, 1,2-dimethyl-, trans-	nd	6698	nd	nd	nd	nd	nd	nd		
Ethanol	1243	4567	nd	nd	nd	nd	nd	nd		

1,3-Butadiene, 2-methyl-	nd	1891	nd	nd	nd	nd	nd	nd	
Propanal	3294	nd	nd	nd	nd	nd	nd	nd	
Acetone	nd	14957	nd	nd	nd	1109	nd	nd	
1,3-Cyclopentadiene	872	5989	nd	nd	nd	nd	nd	1354	± 182
Methyl isocyanide	1138	8055	492	nd	445	nd	nd	1508	± 131
Acrylonitrile	837	nd	nd	nd	nd	nd	nd	1998	± 208
Acetamide, N,N-dimethyl-	nd	4288	378	nd	378	nd	nd	4868	± 361
Total Light Hydrocarbons	135688	732359	195900	200958	80985	117931	97115	91051	

nd: non-detected (<10 ppm)

From **Table 2**, it can be seen that only under pyrolytic conditions was there a hydrogen production increasing the yields with the temperature. This trend was observed by other authors in plastic pyrolysis (Barbarias et al., 2016; Wu and Williams, 2008) at different temperatures. Hydrogen production by endothermic gasification of carbon and reforming of methane and tars could be favored by increasing the temperature, as postulated by He et al.(2009) in an extensive study of syngas production from polyethylene waste. Another important result from the pyrolysis runs is the significant yields of CO and CO_2 detected at all temperatures, which is common in pyrolysis experiments from polymers with a high amount of oxygen in their molecular structure such as non-viscoelastic polyurethanes (Blomqvist et al., 2007; Lönnermark and Blomqvist, 2006), polyester (Moltó et al., 2006) or polycarbonates (Antonakou et al., 2014). The temperature effect was the same for CO and CO_2 with an increase in the formation factor with the temperature; this rise was higher from 750ºC to 850ºC. The evolutions observed for these three compounds (H_2, CO and CO_2) are interrelated bearing in mind that the increase of temperature under pyrolytic conditions mainly produces H_2 and carbon which would react with CO_2 to produce CO (Zhang et al., 2006).

On the other hand, the CO and CO_2 yields obtained in the combustion runs were much higher than those detected in pyrolysis at the same temperature due to the fact that the increase of oxygen content in the atmosphere promoted the fuel combustion. In fact, the combustion efficiency, calculated as the conversion of the C in CO_2, obtained in the combustion experiments was in the

254 range of 55% at 550ºC to 85% at 850ºC. This latter value was in fact similar to that obtained by
255 Zhu et al.(2015) in their study of the emissions from combustion of a high-nitrogen fuel under
256 different oxygen atmospheres in a fluidized bed. In the combustion runs, CO and CO_2 (together)
257 accounted for 95%-96% of all gases and volatile compounds detected at four temperatures
258 dominating the emissions in the same way as other results also obtained during the thermal
259 degradation under oxidative atmosphere of non-viscoelastic polyurethane foams (Bijloos and
260 Lougheed, 2009; Reisen et al., 2014).

261 Regarding the light hydrocarbons detected by GC-FID **Table 2**, ethylene, methane and ethane,
262 in this order were the main products both in the pyrolysis and combustion runs. The total yields
263 in the pyrolysis experiments were higher than those obtained in the combustion runs at the same
264 temperatures, with a maximum at 650ºC under both atmospheres. Acetylene and methane, which
265 are common products of many cracking reactions (Conesa et al., 2009), presented a maximum
266 formation at 850ºC in pyrolysis and combustion, respectively. These compounds have also been
267 previously detected in the thermal degradation of non-viscoelastic polyurethane foams but with
268 different yields and trends due to the emissions depending on the material composition and the
269 experiment conditions (Adeosun, 2014; Bijloos and Lougheed, 2009; Garrido et al., 2016b).

270 Other non-condensable compounds were analyzed by GC-MS and those that presented the
271 highest levels are shown in **Table 2** and the rest are reported in **Table S1** of the Supporting
272 Information. Acetaldehyde was one of the main products detected not only in pyrolysis but also
273 in combustion. This product accounted for 50-81% of the total light hydrocarbons detected in the
274 pyrolysis runs and 53-71% in the combustion experiments at 550ºC, 650ºC and 750ºC.These
275 percentages are similar to those obtained by Reisen et al.(2014) from the combustion of two types
276 of non-viscoelastic polyurethane foams.

277 The total yields of light hydrocarbons (considering those detected by GC-FID and GC-MS) in
278 the pyrolysis runs were, in general, higher than those obtained under an oxidative atmosphere at
279 the same temperature except at 750ºC where the combustion experiment produced an amount of
280 light hydrocarbons slightly higher than the pyrolysis. Total yields presented a maximum at an
281 intermediate temperature of 650ºC in pyrolysis and 750ºC in combustion.

The percentage of N in polyurethane-based materials is usually 5-8%, which is between 1.8 and 150 times higher than that present in common biomass. This fact means that during the thermal degradation of this type of material, compounds like nitric oxide (NO), hydrogen cyanide (HCN) and ammonia (NH_3) reach high levels in the exhaust gases (Guo et al., 2014). Due to their toxicity, the evolution of these products has been analyzed. **Figure 1** shows the evolution curves of yields for HCN (A), NH_3 (B) and NO (C) detected in pyrolysis and combustion runs at different temperatures.

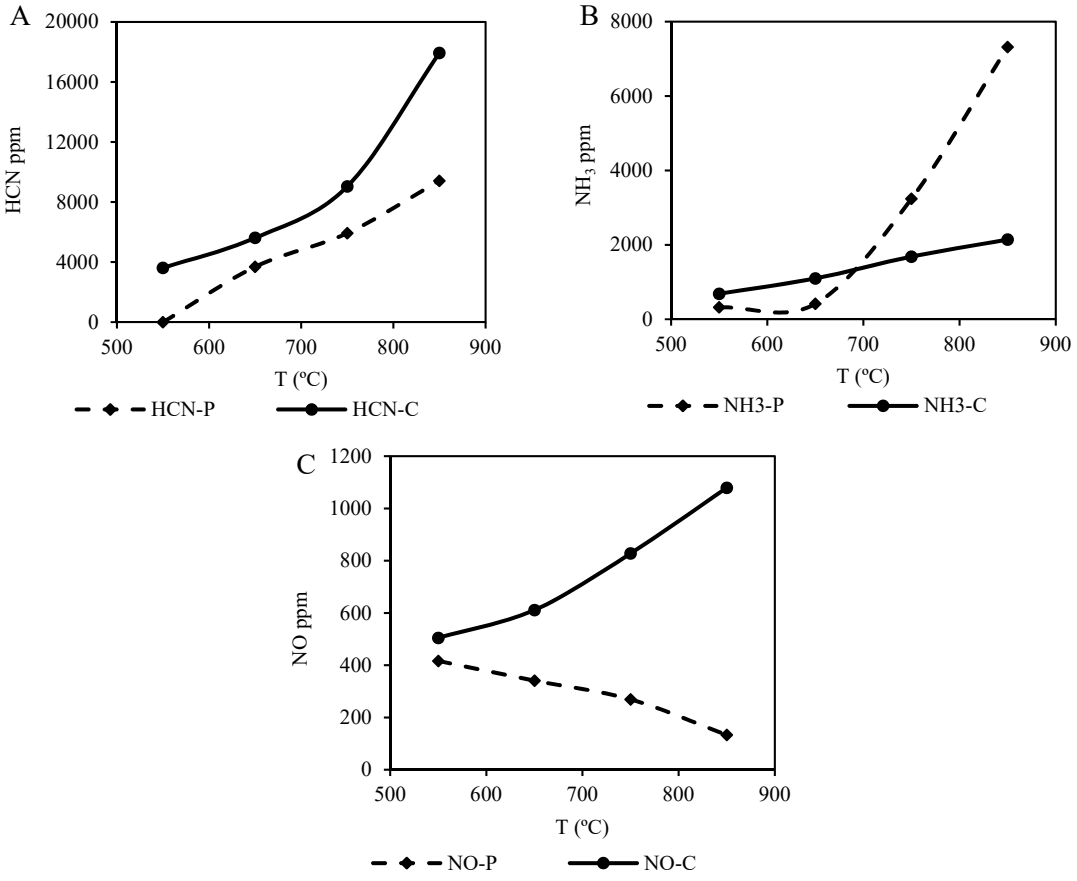

Figure 1. Evolution of HCN (A), NH3 (B) and NO (C) in pyrolysis (P) and combustion (C) experiments at different temperatures.

It can be seen that in combustion and pyrolysis experiments, the main product was HCN, followed by NH_3 and NO (with concentrations up to three orders of magnitude lower than those detected for HCN). This distribution of N-products is common from the thermal degradation of high nitrogen content polymers (Recari et al., 2016).

295 The nitrogen recoveries obtained for each compound were 6-9% in pyrolysis and 6-28% in
296 combustion experiments as HCN (**Figure 1A)**, 1-19% and 4-5% in pyrolysis and combustion as
297 NH_3 (**Figure 1B)**, and 4-1% in pyrolysis and 4-8% in combustion as NO (**Figure 1C).**
298 Analyzing the behavior of each compound separately, it can be seen that HCN yields during
299 pyrolysis were lower than in combustion, which was also detected by other authors (Chang et al.,
300 2004; Lönnermark and Blomqvist, 2006). This fact can be explained bearing in mind that the
301 presence of O_2 promotes the rupture of N-containing structures, allowing the release of HCN from
302 the urethane bond during the combustion (Chang et al., 2004). The effect of temperature was
303 similar in both atmospheres, increasing the yields with temperature. Dagaut et al.(2008)
304 postulated that in nitrogenated materials with a high O/N ratio (as is the case of VMF),
305 temperatures above 750ºC or higher favor the formation of HCN. This explains the great increase
306 from 750ºC to 850ºC observed in **Figure 1A**, not only in combustion but also in the pyrolysis
307 experiments.
308 The second main product was NH_3, which presented a similar trend to HCN, increasing the
309 concentration in the evolved gases with the temperature (**Figure 1B)** in both atmospheres. This
310 coincidence in the evolution of NH_3 and HCN has been reported previously from the gasification
311 of coal (Chang et al., 2004) and from the pyrolysis of some biomasses (rice husk, sawdust and
312 corncob) (Shu et al., 2015). Two different trends can be observed analyzing the effect of the
313 atmosphere. On the one hand, at 550ºC and 650ºC the presence of oxygen favored the NH_3
314 formation by the rupture of the N-containing structures in foam (Chang et al., 2004). However, a
315 temperature increase in pyrolysis runs produced around 3 times more NH_3 than in the combustion
316 runs. This indicates that at high temperatures, the NH_3 formation occurs by hydrogenation by the
317 H radicals of N-sites present in the fuel (Tian et al., 2013), which is confirmed observing the great
318 amount of H_2 produced in pyrolysis at 850ºC (**Table 2**).
319 Finally, observing **Figure 1C,** it can be seen that the levels of NO detected in combustion
320 experiments were higher than those obtained under an inert atmosphere, according to the results
321 reported by other authors from the pyrolysis and combustion of high nitrogen content polymers
322 (Guo et al., 2016). This fact can be explained bearing in mind that the high levels of HCN and

323 NH_3 in combustion experiments, due to the ammonia and hydrogen cyanide, can secondarily react
324 with oxygen or oxygen free radicals, producing NOx (Guo et al., 2016). Also, the increase of the
325 temperature together with the presence of O_2 allowed the release of nitrogen species from fuels,
326 mainly HCN in the case of VMF, to intensify and further their conversion into NO (Zhang et al.,
327 2006; Zhu et al., 2015).

328 Regarding the pyrolysis results, the decrease of NO and the increase of NH_3 with the
329 temperature are closely related. The volatiles emitted from pyrolysis of N-containing materials
330 contain hydrocarbons and reducing nitrogenous components (such as NH_3 and HCN) in high
331 concentration that can form a reducing atmosphere. Under these conditions, NO reacts with
332 radicals of light hydrocarbons (methane, acetylene, ethylene and ethane) reducing the emission
333 of this compound (Shu et al., 2015) (**Figure 1B and C)**.

334 ### 3.2.PAHs and other semivolatile compounds.

335 **Table S2** (Supporting Information) presents the yields of the 16 priority PAHs listed as
336 hazardous air pollutants by the Environmental Protection Agency (1998) together with the other
337 semivolatile compounds analyzed in SCAN mode. In the blank experiments, the yields detected
338 were lower than 2 ppm, which was the value of the detection limit calculated from the lowest
339 calibration point. The LOD for semivolatile compounds analyzed in SCAN mode has been
340 calculated considering the lowest calibration point of 16 priority PAH, obtaining yields in the
341 range of 2-10 ppm. The selected LOD value was 10 ppm.

342 **Figure 2** shows the emission levels of the five major compounds detected in the pyrolysis and
343 combustion experiments. Naphthalene was the most important PAH detected in almost all
344 conditions except in pyrolysis at 550ºC where fluorene was the main product. The predominance
345 of naphthalene in the condensable products from the thermal degradation is common for high N-
346 containing fuels (Ayanoğlu and Yumrutaş, 2016; Yang et al., 2012). Following naphthalene, other
347 PAHs such as acenaphthylene, fluorene, phenanthrene and anthracene were also detected at high
348 levels, in such a way that in all experiments, the contribution of these five compounds to total
349 yields was approximately 90%.

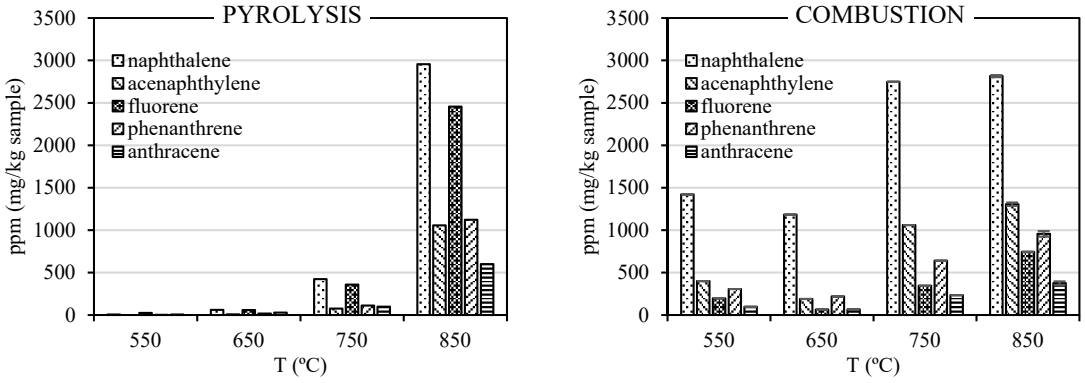

Figure 2. Main PAHs detected in pyrolysis and combustion experiments at different temperatures.

Tomas and Wornat (2008) found that an inert atmosphere and temperatures higher than 800ºC were the best conditions to achieve a significant production of PAHs, which agrees with the results presented in the present work where the maximum formation was obtained in pyrolysis at 850ºC (**Table S2**). The total yield increased more than 197 times in pyrolysis experiments from 550ºC to 850ºC, mainly due to the contribution of 2 and 3-ring PAHs, which was consistent with the study developed by Terakado et al.(2014).

In combustion, it can be seen that at lower temperatures (< 850ºC), the presence of oxygen resulted in an increase in the PAH levels, due to the production of hydrogen atoms and radicals involved in the PAH formation (Sánchez et al., 2013; Schuetzle et al., 2015). A similar trend as in pyrolysis was obtained in the combustion experiments with a rise of PAH with the temperature. Combustion at 850ºC produced 4 times more PAH than combustion at 650ºC (lowest level) (**Table S2**), close to the relation obtained from the incineration at different temperatures of acrylic waste (Singh and Prakash, 2007).

From the 16 priority PAHs, benzo[a]pyrene (B[a]P) is the only PAH classified as carcinogenic to humans by the IARC (International Agency for Research on Cancer) (Sarigiannis et al., 2015). In order to assess the toxicity of the PAH mixtures obtained in each experiment, the total carcinogenic potency has been calculated according to Eq. (1)

$$B[a]P_e = \sum_{i=1}^{16} C_i \times TEF_i \quad (1)$$

where $B[a]P_e$ is the carcinogenic potency referred to B[a]P equivalent concentration, C_i is the concentration of each PAH congener and TEF is the toxic equivalent factor for each PAH provided by Nisbet and LaGoy (1992) (Mohammed et al., 2016; Pongpiachan et al., 2015). Results are shown in **Figure 3** with the total PAH yields.

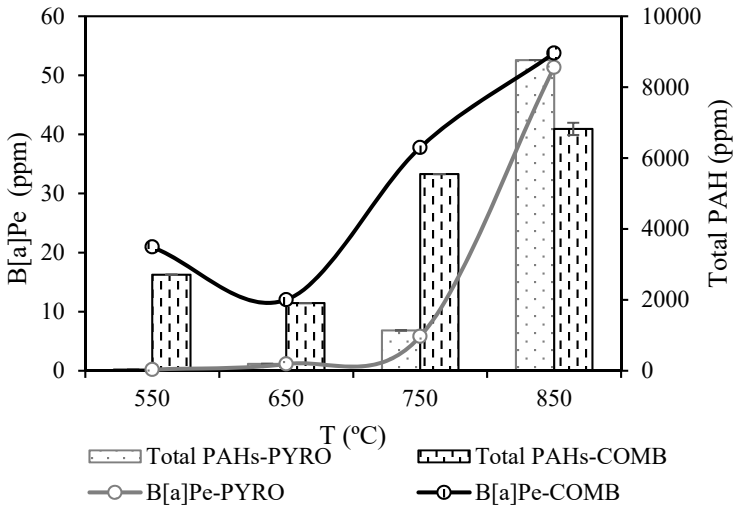

Figure 3. Toxicity (as B[a]Pe) and total PAH yields from the pyrolysis and combustion of VMF at 550, 650, 750 and 850ºC.

From **Figure 3**, it can be seen that the toxicity follows the same trend as the total yields. The B[a]Pe levels of the combustion runs at 550ºC, 650ºC and 750ºC are higher than those calculated in pyrolysis at the same temperatures. In spite of the greater PAH production in pyrolysis at 850ºC, the gases evolved in combustion at 850ºC presented similar carcinogenic potency due to the difference in yields of benzo[a]pyrene from pyrolysis to combustion (**Table S2**).

Blomqvist et al. (2014) performed a series of degradation experiments in a steady-state tube furnace at different conditions employing PVC carpet and wood board as materials for the analysis of the PAHs formation. In an under-ventilated condition, which is similar to the combustion experiments developed in the present work, they found that PVC carpet emitted around 100 B[a]Pe ppm, whereas for wood board the level decreased up to 10 B[a]Pe ppm as was expected bearing in mind that synthetic polymers produce much more amount of PAHs than natural materials (Conesa et al., 2009). It is important to remark that the highest toxicity level detected from the degradation of viscoelastic memory foam waste (54 ± 4 B[a]Pe ppm in combustion at 850ºC) was lower than that analyzed from the combustion of bituminous coal in a

coal-stove (134.5 B[a]Pe ppm) (Liu et al., 2009). This coal accounts for about 70-80% of fuel consumption in China (Wu and Wei, 2015).

A total number of 137 other semivolatile compounds was detected by GC-MS with accuracy higher than 80% (**Table S2).** Total yields increased with the temperature both in the pyrolysis and combustion experiments, in the same way that Watanabe et al. (2007) found during the thermal degradation of different plastics in the range of 70-300ºC. The standard deviations calculated from the two duplicates of combustion experiments at 850ºC are relatively low and only the compounds detected at low-lying levels presented standard deviations up to 28%.

Aniline, benzonitrile and acridine were the most important products in all experiments (**Table S2).** One of the most abundant products in the pyrolysis experiments was o-Toluidine (**Table S2)** which is a nitrogen derivate aromatic compound that should release directly from the long polymer chains. This hypothesis can be confirmed bearing in mind the relationship between the molecular structure of 2,4-TDI (Toluene diisocyanate) and 2,6-TDI, which are the most common monomers in polyurethane and viscoelastic memory foam production (Mark, 2013) and the molecular structure of o-Toluidine. The structures of 2,4-TDI, 2,6-TDI and o-Toluidine are presented in **Figure 4**.

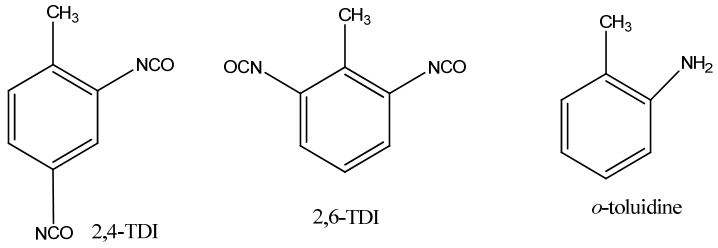

Figure 4. Molecular structure of 2,4-TDI, 2,6-TDI (monomers of polyurethane foams) and o-Toluidine (semivolatile compound detected).

N-containing compounds represent around 60% of the total semivolatile compounds detected with nitrogen, mainly, as nitrile or amine functional groups bonded to aromatic rings. Aniline, benzonitrile and acridine accounted for about 20-50% of the total N-containing semivolatile compounds obtained in all experiments.

In addition to the results shown for each compound, a carbon balance was carried out considering the carbon contained in the gases, volatile and semivolatile compounds as well as in

415 the initial sample and that remaining in the ash (analyzed by elemental analysis). The recoveries
416 of carbon obtained were 37, 84, 68 and 73% for pyrolysis at 550, 650, 750 and 850ºC respectively.
417 The low value obtained at 550ºC can be explained bearing in mind that in the pyrolysis experiment
418 at 550ºC, there were a lot of peaks that were not identified and quantified because they did not
419 present an accuracy higher than 80%. In the same way, in all runs, there were non-collected tars
420 and consequently, the C balances were less than 100%.

421 The recoveries obtained in combustion experiments were 87% at 550ºC, 106% at 650ºC, 108%
422 at 750 and 110% ± 3% at 850ºC. The values higher than 100% were obtained in the combustion
423 at highest temperatures where CO_2 and CO were the main products, so the error should come
424 from the GC analysis. On the other hand, the lowest recovery at 550ºC can be a consequence of
425 the non-collected tars formed at low temperatures. Despite this value, really good recoveries were
426 achieved in all experiments.

427 In the same way, the oxygen balance was also performed, but in this case only for the pyrolysis
428 experiments due to the fact that in the combustion experiments the oxygen introduced into the
429 reactor as carrier gas reacts with the sample, so the recoveries cannot be calculated. At 550, 650,
430 750 and 850 ºC in pyrolysis, the oxygen recoveries were 39%, 88%, 64%, and 63%, also the
431 lowest temperature presented the lowest recovery. Note that water was not analyzed and there can
432 also be some oxygenated non-collected tars which have not been considered in the balance.

433 ### 3.3.Chlorinated benzenes and chlorinated phenols.

434 Following the same procedure described for PAHs, the LODs of chlorinated benzenes (ClBzs)
435 and phenols (ClPhs) were calculated considering the first point in the calibration curves, obtaining
436 LODs of 0.11 and 0.03 ppm for ClBzs and ClPhs, respectively. The concentration of blanks was
437 below the first point of the calibration curve.

438 A relatively low amount of chlorinated benzenes (ClBzs) was obtained (**Table S3** in Supporting
439 Information). The experiment which presented the highest total yields of 0.57 ppm was pyrolysis
440 at 850ºC. The only congener evolved was mono-ClBz in all experiments except in pyrolysis at
441 550ºC where no emissions were detected. In pyrolysis conditions, a clear increase of the mono-
442 ClBz yield with the temperature was observed, whereas in combustion no clear trend was found.

The yields of the congener specific analysis of chlorinated phenols (ClPhs) for all runs are shown in **Table S4** (Supporting Information). The highest yields were observed at 850ºC, being slightly higher in pyrolytic than in oxidative conditions, consistent with the profile of PAHs. Similar behavior with the temperature was observed in both the presence of and absence of oxygen, increasing the total yields when increasing temperature.

Regarding the specific congener profiles, **Figure 5** shows the results (% relative) of the compounds detected in the pyrolysis and combustion experiments at 550, 650, 750 and 850ºC. Monochlorinated phenols (3-+4-) were the most abundant products at all temperatures studied which agrees with the results obtained by Kaivosoja et al. (2012) in their study about the emissions from residential wood combustion. In pyrolysis, 3,4,5-TriClPh was also obtained at a relative high formation factor.

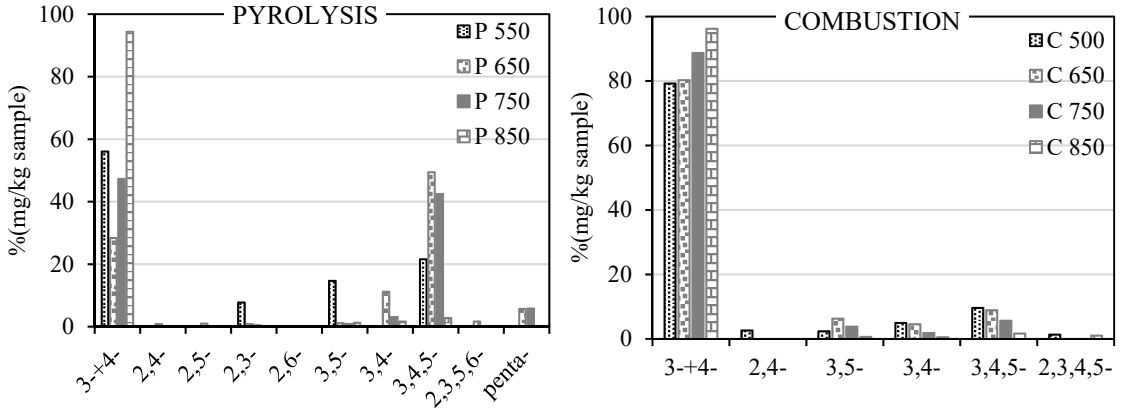

Figure 5. Congener profiles of chlorinated phenols during pyrolysis (P) and combustion (C) of viscoelastic memory foam (VMF) at four different temperatures (550, 650, 750 and 850ºC (average value from duplicates runs)).

It is interesting to observe that the total yields of ClPhs were much higher than the ClBzs in the same conditions, which was the expected trend taking into account that ClPhs can probably be formed from ClBzs by oxidation and reaction with an·OH radical (Ballschmiter et al., 1988).

3.4.PCDD/Fs and dl-PCBs

The integration of samples to analyze PCDD/Fs and dl-PCBs was performed employing the Masslynx data system (v.4), which calculates the detection limit (LOD) for each congener in each sample defined as a signal/noise ratio equal to 3 (Blanchet-Letrouvé et al., 2014). It is assumed

that all non-detected compounds present yields equal or lower than LOD. The ranges of LOD obtained were 0.2-9.3 ppt for PCDD/Fs and 0.1-7.5 ppt for dl-PCBs. The blank experiments performed throughout the study, before each experiment, were integrated and subtracted from the levels obtained in the experiments. No emission was observed in the PCDD/Fs blank experiments, whereas some dl-PCB congeners were detected (**Table S6, Supporting Information**).

Table 3 shows the PCDD/Fs and dl-PCBs emissions from pyrolysis (P) and combustion (C) of viscoelastic memory foam (VMF) at 550, 650, 750 and 850ºC (duplicate). Apart from the yields of the 17 isomers of 2,3,7,8-substituted PCDD/F and 12 mono-ortho and non-ortho dl-PCBs, the toxicities of the samples, expressed in terms of TEQ, have also been calculated in the same way as for 16 priority PAHs. Two different toxic equivalent factors were employed for PCDD/F, I-TEF-1988 (NATO/CCMS, 1988) and WHO-TEF-2005 (Van den Berg et al., 2006), whereas for dl-PCBs the toxicities were evaluated with WHO-TEF-2005.

Table 3. Emissions of PCDD/Fs and dl-PCBs from pyrolysis (P) and combustion (C) runs of VMF at different temperatures.

COMPOUND	ppt (pg/g sample)								
	P 550	P 650	P 750	P 850	C 550	C 650	C 750	C 850	σ
PCDD/Fs									
2378-TCDF	nd	nd	nd	nd	1.3	3.3	2.2	nd	
12378-PeCDF	2.7	2.0	1.8	nd	0.9	1.2	0.9	5.1	± 0.3
23478-PeCDF	3.3	1.3	1.7	nd	nd	1.5	1.2	5.0	± 0.1
123478-HxCDF	nd	2.6	2.1	nd	1.0	0.7	1.1	13.4	± 1.5
123678-HxCDF	nd	1.6	2.3	nd	nd	0.8	1.3	14.7	± 1.8
234678-HxCDF	nd	3.4	3.3	nd	1.6	0.6	1.7	17.3	± 4.6
123789-HxCDF	5.7	nd	2.7	nd	1.1	0.7	1.7	17.9	± 3.0
1234678-HpCDF	6.0	5.5	2.8	nd	nd	3.5	4.3	28.7	± 2.9
1234789-HpCDF	nd	7.1	1.8	nd	nd	3.0	4.3	28.2	± 2.5
OCDF	7.7	16.8	50.0	nd	nd	6.1	10.3	79.3	± 4.3
2378-TCDD	nd	nd	1.4	nd	nd	nd	1.0	nd	
12378-PeCDD	nd	nd	1.8	nd	nd	2.4	0.9	5.5	± 0.6
123478-HxCDD	nd	nd	4.1	nd	nd	nd	1.5	19.5	± 1.6
123678-HxCDD	nd	5.2	nd	nd	nd	4.0	1.5	20.6	± 0.7
123789-HxCDD	4.2	14.0	3.6	nd	nd	3.1	1.4	20.2	± 2.1
1234678-HpCDD	nd	13.4	7.8	nd	nd	nd	3.6	37.3	± 3.9
OCDD	20.9	70.2	168.6	nd	nd	12.0	16.9	102.0	± 0.8
Total PCDF	25.4	40.3	68.5	nd	5.9	21.5	29.1	209.4	± 20.5
Total PCDD	25.1	102.8	187.3	nd	nd	21.5	26.7	205.1	± 0.6

sum PCDD/F	50.5	143.1	255.8	nd	5.9	43.0	55.8	414.5	± 21
Total WHO-TEQ PCDD/F	2.1	3.4	5.7	<0.3	0.5	4.3	3.7	20.5	± 2.3
Total I-TEQ PCDD/F	2.8	3.8	5.4	<0.2	0.5	3.4	3.5	19.0	± 2.0
dl-PCBs									
PCB-81	5.4	7.7	3.7	0.9	nd	2.1	1.8	1.7	± 0.1
PCB-77	33.3	59.0	34.8	4.7	15.3	10.3	7.2	5.9	± 0.7
PCB-123	17.1	31.9	18.9	2.3	6.8	4.3	4.9	2.2	± 0.4
PCB-118	145.5	228.2	72.9	5.1	50.7	23.2	28.4	14.5	± 1.3
PCB-114	4.9	5.8	1.5	2.6	2.0	1.2	1.0	0.6	± 0.1
PCB-105	49.4	77.3	18.7	0.5	17.9	6.2	2.3	2.6	± 0.6
PCB-126	1.9	3.3	2.9	0.5	1.1	0.9	0.5	0.9	± 0.1
PCB-167	9.4	18.0	5.6	0.6	2.8	0.9	nd	2.0	± 0.7
PCB-156	9.8	14.1	5.2	0.7	2.5	1.6	1.3	2.2	± 0.4
PCB-157	1.7	3.3	1.8	0.3	0.5	0.4	0.3	nd	± nd
PCB-169	0.5	0.7	0.5	nd	nd	nd	0.3	nd	± nd
PCB-189	nd	2.2	0.5	0.9	0.7	nd	nd	nd	± nd
sum dl-PCBs	*279.0*	*451.7*	*167.0*	*19.1*	*100.2*	*51.1*	*48.0*	*32.6*	*± 0.5*
Total WHO-TEQ dl-PCBs	0.22	0.37	0.31	0.05	0.11	0.09	0.06	0.09	± 0.01
Total WHO-TEQ (PCDD/F+dl-PCBs)	2.34	3.81	6.05	<0.25	0.64	4.59	3.71	20.58	± 0.98

The concentration of PCDD/F congeners in the different runs varied over of three orders of magnitude, ranging from 0.6 to 168.6 pg/g sample. The pyrolysis experiments presented higher yields than the combustion experiments at 550ºC (50.5 vs. 5.9 pg/g sample), 650ºC (143.1 vs. 43.0 pg/g sample) and 750ºC (255.8 vs. 55.8 pg/g sample), whereas at 850ºC this trend reversed; combustion at 850ºC was the condition where more PCDD/Fs were formed (414.5 ± 21 pg/g sample) and in pyrolysis at 850ºC no PCDD/Fs were detected.

In the pyrolysis runs, the increase of the temperature involved a higher production of PCDD/Fs up to 750ºC and total or near total destruction at 850ºC. This trend is in accordance with the phenomena observed by Evan (2004) in the study of PCDD/Fs evolved during the pyrolysis of 2-Chlorophenol and 2-Bromophenol in a similar quartz reactor to that employed in this research and in a temperature range of 300-1000ºC. She found a gradual increase of the PCDD/F formation from 300 to 750ºC and at temperatures higher than 750ºC the PCDD/F yields decreased achieving

492 the destruction of 99% of the PCDD/Fs at 850ºC. The hydrogen atom probably could be the
493 dominant reactive radical in the PCDD/F formation (Evans, 2004) coinciding with a greater H_2
494 generation (**Table 2**), except at 850ºC where the great amount of NH_3 detected seems to be
495 responsible for the inhibition of the PCDD/F formation as reported previously (Chen et al., 2015;
496 Zhan et al., 2016). Dai et al. (2013) developed a study of PCDD/Fs evolved during a conventional
497 pyrolysis of wet sewage sludge in the temperature range of 400-600ºC, finding an increase of the
498 amount of PCDD/Fs in the gas phase with the temperature.

499 In the combustion runs, a gradual increase of PCDD/F total yields was obtained from 550ºC to
500 750ºC while from 750ºC to 850ºC the PCDD/F formation was multiplied 7.5 times. This great
501 difference in the emissions from low to high temperature combustion was also observed by other
502 authors from the decomposition of different material such as polyvinyl chloride (Aracil et al.,
503 2005) or polychloroprene (Aracil et al., 2010) in the same furnace employed in the present study.

504 Combustion at 850ºC presented the highest toxicity level (20.5 ± 2.3 pg WHO-TEQ/g sample
505 and 19.0 ± 2.0 pg I-TEQ/g sample), whereas at 850ºC in pyrolysis the levels shown in **Table 3**
506 have been calculated considering the LOD values due to no congener being detected.

507 The maximum level registered in this work is lower than those detected from the combustion
508 of other polymeric materials and biomass products indicated in **Table 4**

509 **Table 4.** Comparison of PCDD/F toxicity levels obtained in the combustion of different
510 materials

Material	Process	Toxicity (pg I-TEQ/g sample)	Reference
VMF	Combustion 850ºC	19.0 ± 2.0	This work
FPUF	Combustion 850ºC	80 ± 17	Garrido et al. (2016b)
ASR	Combustion 850ºC	212	Edo et al. (2013)
PVC carpet	Under-ventilated combustion (R_{CO}≈0.13)	174	Stec et al. (2013)
Tomato plant	Combustion	105.35	Moltó et al. (2010)
Sugarcane	Burn	252.6	Gullett et al. (2006)
PS		21	
PE	Combustion	73	Katami et al. (2002)
PET		32	

511

512 Flexible polyurethane foam (FPUF) (which presents a similar composition of VMF) produced
513 a slightly higher level than that obtained from VMF during the combustion at 850ºC in the same
514 tubular reactor (Garrido et al., 2016b). The difference observed in the toxicity of some of the
515 materials presented in **Table 4** could be explained bearing in mind that the PCDD/F formation
516 depends on multiple factors such as fuel, temperature and the Cl^- content (Zhang et al., 2008).
517 The Cl^- content of FPUF, VMF and ASR (material with around 35% of polymers) is 253, 117 and
518 8013 mg Cl^-/kg sample, where ASR presents a concentration one order of magnitude higher than
519 the other two materials. Nevertheless, for ASR the presence of Fe and Cu (not detected in VMF
520 and FPUF) can also promote the PCDD/F formation. The low I-TEQ and WHO-TEQ levels of
521 the VMF were a consequence of the small amount of 2378-TCDD congener (which is the most
522 toxic one) detected in all samples (**Table 3**).
523 In the pyrolysis runs, the predominant congener was OCDD (42%, 49% and 66% at 550, 650
524 and 750ºC, respectively) followed by OCDF (15%, 12% and 20% at 550, 650, and 750ºC,
525 respectively) and the other higher chlorinated isomers of both PCDDs and PCDFs were also
526 formed in a higher amount than the lower ones, mainly at 750ºC. This behavior agrees with the
527 hypothesis that under inert atmosphere chlorination reactions dominate producing mainly high
528 chlorinated congeners (Altarawneh et al., 2009).
529 In combustion at 550ºC, no PCDDs were obtained and HxCDFs were the predominant
530 congeners. The increase of the temperature involved an increase in the amount of high chlorinated
531 congeners in the way that at 850ºC OCDF and OCDD accounted for 19.1% ± 0.1% and 24.7% ±
532 1.1% of total emission, respectively. The predominance of the hepta- and octa-CDD/Fs in
533 combustion experiments at temperatures from 650ºC to 850ºC is similar to that observed from the
534 open burning of a residential waste dump (Gullett et al., 2010) or from the combustion of artificial
535 municipal solid waste in a laboratory scale reactor (Jansson et al., 2009). Furthermore, the
536 combustion of a mobile phone case at 850ºC in the same reactor employed in the present work
537 (Moltó et al., 2011) presented similar behavior. These facts suggest that the PCDD/F patterns
538 could not be directly related to the fuel type or operating conditions and probably some

539 thermodynamics constraints should dictate the formation of PCDD/F congeners (Gullett et al.,
540 2010).

541 In relation to the emission of dl-PCBs, in **Table 3**, it can be seen that, in the same way as
542 PCDD/Fs, pyrolysis experiments produced higher levels than combustion experiments at 550ºC,
543 650ºC and 750ºC, deducing that the presence of oxygen in the atmosphere involved a reduction
544 in the total yields of 64%, 89% and 71%, respectively. Nevertheless, at 850ºC the combination of
545 high temperature and oxidative atmosphere contributed to the formation of dl-PCBs, 32.6±0.5
546 pg/g sample in combustion at 850ºC versus 19.1 pg/g sample in pyrolysis at 850ºC. Molto et
547 al.(2009) also found that the pyrolysis of electronic waste at 500ºC performed in the same reactor
548 used in the present work produced higher dl-PCB yields than combustion, whereas at 850ºC the
549 trend turned upside down (Moltó et al., 2011).

550 Regarding the effect of temperature, a maximum level of total yields was detected at
551 intermediate temperature (650ºC) in the pyrolysis experiments with an important decrease from
552 750ºC to 850ºC the same as that obtained in PCDD/Fs. On the contrary, in combustion the
553 opposite behavior of dl-PCBs and PCDD/Fs was observed with a minimum and a maximum
554 value, respectively, at 850ºC.

555 **Figure 6** shows the congener profiles of 6 predominant dl-PCBs in the emission from pyrolysis
556 and combustion of VMF, which accounted for 73%-94% of the total yields detected in the
557 experiments. PCB-118, PCB-77 and PCB-105 were the most abundant congeners in all runs,
558 followed by PCB-123 and PCB-81. In comparison with other results, Garrido et al.(2016b) found
559 that PCB congeners 118, 77 and 105 were also the most abundant ones from the pyrolysis and
560 combustion of flexible polyurethane foam (FPUF) at 550 and 850ºC, and Molto et al.(2009)
561 obtained a similar congener profile during the pyrolysis and combustion of electronic waste (EW)
562 at 500ºC. From these three materials, the highest dl-PCB total yields were obtained in the
563 degradation of EW followed by FPUF and VMF. This is probably a consequence of the chlorine
564 content in the wastes, which was 400, 253 and 117 mg/kg sample, respectively.

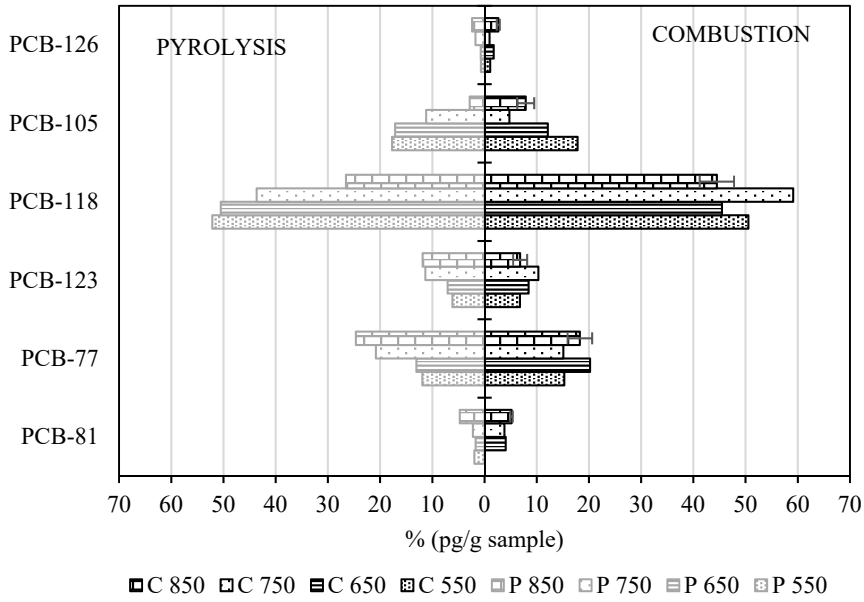

565

566 **Figure 6.** dl-PCB congener profiles obtained in pyrolysis (P) and combustion (C) experiments
567 at four different temperatures (550, 650, 750 and 850ºC)

568 The toxicity levels due to dl-PCBs in the pyrolysis experiments were in the range 0.05-0.37 pg
569 WHO-TEQ/g, but in combustion, this was reduced to 0.06-0.11 pg WHO-TEQ/g. Analyzing the
570 amount of congeners shown in **Figure 6**, it could be said that PCB-126 was the dl-PCBs that
571 mostly contributed to the toxicity levels, bearing in mind that this congener is the most toxic
572 (WHO-TEF equal to 0.1).

573 ## 4. Conclusions

574 In this study, the emission from the thermal degradation of viscoelastic memory foam under
575 different conditions has been developed. The experiment performed under an inert atmosphere at
576 850ºC favors the formation of semivolatile compounds such as PAHs, but the levels obtained of
577 these products do not present a risk due to their low toxicity. Also, in pyrolysis at 850ºC, NH_3
578 presents the maximum emissions, which probably produces the inhibition of the PCDD/F
579 formation. On the other hand, also pyrolysis, but in this case at 650ºC, is the best condition to
580 produce a great amount of light hydrocarbons like methane and ethylene and dl-PCBs.

581 Compounds like hydrogen cyanide (HCN) and nitric oxide (NO) are emitted mainly in
582 combustion at 850ºC, the same as PCDD/Fs that present a toxicity level much lower than that
583 found from the combustion of some biomasses or other plastics like PE and PET.

584 It must be emphasized that the most important problem to deal with in the incineration of VMF
585 should be the NO and HCN emissions, so it will be necessary at least to consider their destruction
586 in subsequent stages.
587 Only for NO, are there regulated limits for its emissions. The levels of the NO formation
588 measured in this research exceed by far the limit level of 400 mg/Nm^3 proposed in the Directive
589 2010/75/EU (European Commission, 2010) for an average daily emission of waste incineration
590 plants, as was expected due to the sub-stoichiometric conditions employed in this study.
591

592 ## Acknowledgment

593 Support for this work was provided by the Spanish Ministry of Culture and Sport and by
594 the CTQ2013-41006-R project from the Ministry of Economy and Competitiveness
595 (Spain) and the PROMETEOII/2014/007 project from the Valencian Community
596 Government (Spain).

597 ## References

598 Adeosun DO. Analysis of Fire Performance, Smoke Development and Combustion Gases from
599 Flame Retarded Rigid Polyurethane Foams. University of Waterloo, 2014.

600 Altarawneh M, Dlugogorski BZ, Kennedy EM, Mackie JC. Mechanisms for formation,
601 chlorination, dechlorination and destruction of polychlorinated dibenzo-p-dioxins and
602 dibenzofurans (PCDD/Fs). Progress in Energy and Combustion Science 2009; 35: 245-
603 274.

604 Antonakou EV, Kalogiannis KG, Stefanidis SD, Karakoulia SA, Triantafyllidis KS, Lappas AA,
605 et al. Catalytic and thermal pyrolysis of polycarbonate in a fixed-bed reactor: The effect of
606 catalysts on products yields and composition. Polymer Degradation and Stability 2014;
607 110: 482-491.

608 Apichatachutapan W, Neff R, Mullins J, Smiecinski TM, Lee TB. Viscoelastic polyurethane
609 foam. Google Patents, 2007.

610 Aracil I, Font R, Conesa JA. Semivolatile and volatile compounds from the pyrolysis and
611 combustion of polyvinyl chloride. Journal of Analytical and Applied Pyrolysis 2005; 74:
612 465-478.

613 Aracil I, Font R, Conesa JA. Chlorinated and Nonchlorinated Compounds from the Pyrolysis and
614 Combustion of Polychloroprene. Environmental Science & Technology 2010; 44: 4169-
615 4175.

616 Ayanoğlu A, Yumrutaş R. Production of gasoline and diesel like fuels from waste tire oil by using
617 catalytic pyrolysis. Energy 2016; 103: 456-468.

618 Ballschmiter K, Braunmiller I, Niemczyk R, Swerev M. Reaction pathways for the formation of
619 polychloro-dibenzodioxins (PCDD) and —dibenzofurans (PCDF) in combustion
620 processes: II. Chlorobenzenes and chlorophenols as precursors in the formation of
621 polychloro-dibenzodioxins and —dibenzofurans in flame chemistry. Chemosphere 1988;
622 17: 995-1005.

623 Barbarias I, Lopez G, Alvarez J, Artetxe M, Arregi A, Bilbao J, et al. A sequential process for
624 hydrogen production based on continuous HDPE fast pyrolysis and in-line steam
625 reforming. Chemical Engineering Journal 2016; 296: 191-198.

626 Bijloos M, Lougheed G. Smoldering of a flexible polyurethane foam sofa. Institute for Research
627 in Construction, National Research Council Canada, Ottawa, Canada. NRCC-50572 2009.

628 Blanchet-Letrouvé I, Zalouk-Vergnoux A, Vénisseau A, Couderc M, Le Bizec B, Elie P, et al.
629 Dioxin-like, non-dioxin like PCB and PCDD/F contamination in European eel (Anguilla
630 anguilla) from the Loire estuarine continuum: Spatial and biological variabilities. Science
631 of The Total Environment 2014; 472: 562-571.

632 Blomqvist P, Hertzberg T, Tuovinen H, Arrhenius K, Rosell L. Detailed determination of smoke
633 gas contents using a small-scale controlled equivalence ratio tube furnace method. Fire and
634 materials 2007; 31: 495-521.

635 Blomqvist P, McNamee MS, Stec AA, Gylestam D, Karlsson D. Detailed study of distribution
636 patterns of polycyclic aromatic hydrocarbons and isocyanates under different fire
637 conditions. Fire and Materials 2014; 38: 125-144.

638 Conesa JA, Font R, Fullana A, Martín-Gullón I, Aracil I, Gálvez A, et al. Comparison between
639 emissions from the pyrolysis and combustion of different wastes. Journal of Analytical and
640 Applied Pyrolysis 2009; 84: 95-102.

641 Consumer Product Safety Commision. Final Rule: Standard for the Flammability (Open Flame)
642 of Mattress Sets. 16 CFR Part 1633 Federal Register Vol. 71, United States, 2006, pp. 52.

643 Couto N, Silva VB, Bispo C, Rouboa A. From laboratorial to pilot fluidized bed reactors: Analysis
644 of the scale-up phenomenon. Energy Conversion and Management 2016; 119: 177-186.

645 Chang L-P, Xie K-C, Li C-Z. Release of fuel-nitrogen during the gasification of Shenmu coal in
646 O2. Fuel Processing Technology 2004; 85: 1053-1063.

647 Chen T, Zhan M-X, Lin X-Q, Fu J-Y, Lu S-Y, Li X-D, et al. PCDD/Fs inhibition by sludge
648 decomposition gases: effects of sludge dosage, treatment temperature and oxygen content.
649 Aerosol Air Qual Res 2015; 15: 702-711.

650 Dagaut P, Glarborg P, Alzueta MU. The oxidation of hydrogen cyanide and related chemistry.
651 Progress in Energy and Combustion Science 2008; 34: 1-46.

652 Dai Q, Jiang X, Wang F, Chi Y, Yan J. PCDD/Fs in wet sewage sludge pyrolysis using
653 conventional and microwave heating. Journal of Analytical and Applied Pyrolysis 2013;
654 104: 280-286.

655 Edo M, Aracil I, Font R, Anzano M, Fullana A, Collina E. Viability study of automobile shredder
656 residue as fuel. J Hazard Mater 2013; 260: 819-24.

657 European Commission. DIRECTIVE 2010/75/EU OF THE EUROPEAN PARLIAMENT AND
658 OF THE COUNCILof 24 November 2010 on industrial emissions (integrated pollution
659 prevention and control) (Recast) (Text with EEA relevance). In: European Commission,
660 editor, DOUE L 334-17, 2010, pp. 17-119.

661 European Commission. COM(2014) 397 final: Proposal for a Directive of the European
662 Parliament and of the Council amending Directives 2008/98/EC on waste, 94/62/EC on
663 packaging and packaging waste, 1999/31/EC on the landfill of waste, 2000/53/EC on end-
664 of-life vehicles, 2006/66/EC on batteries and accumulators and waste batteries and
665 accumulators, and 2012/19/EU on waste electrical and electronic equipment., 2014.

666 European Communities. Directive 2000/76/EC of the European Parliament and of the Council of
667 4 December 2000 on the incineration of waste. Official Journal of the European
668 Communities 2000; 332.

669 Evans CS. Comparison studies of the mechanistic formation of polyhalogenated dibenzo-p-
670 dioxins and furans from the thermal degradation of 2-bromophenol and 2-chlorophenol.
671 Faculty of the Louisiana State University and Agricultural and Mechanical College in
672 partial fulfilment of the requirements for the degree of Doctor of Philosophy in The
673 Department of Chemistry by Catherine Spearing Evans BS, University of the South,
674 Sewanee, 2004.

675 Font R, Gálvez A, Moltó J, Fullana A, Aracil I. Formation of polychlorinated compounds in the
676 combustion of PVC with iron nanoparticles. Chemosphere 2010; 78: 152-159.

677 Font R, Moltó J, Egea S, Conesa JA. Thermogravimetric kinetic analysis and pollutant evolution
678 during the pyrolysis and combustion of mobile phone case. Chemosphere 2011; 85: 516-
679 524.

680 Garrido MA, Font R, Conesa JA. Kinetic study and thermal decomposition behavior of
681 viscoelastic memory foam. Energy Conversion and Management 2016a; 119: 327-337.

682 Garrido MA, Font R, Conesa JA. Pollutant emissions during the pyrolysis and combustion of
683 flexible polyurethane foam. Waste Management 2016b; 52: 138-146.

684 Gullett BK, Touati A, Huwe J, Hakk H. PCDD and PCDF Emissions from Simulated Sugarcane
685 Field Burning. Environmental Science & Technology 2006; 40: 6228-6234.

686 Gullett BK, Wyrzykowska B, Grandesso E, Touati A, Tabor DG, Ochoa GS. PCDD/F, PBDD/F,
687 and PBDE Emissions from Open Burning of a Residential Waste Dump. Environmental
688 Science & Technology 2010; 44: 394-399.

689 Guo X, Wang L, Li S, Tang X, Hao J. Gasification of waste rigid polyurethane foam: optimizing
690 operational conditions. Journal of Material Cycles and Waste Management 2015; 17: 560-
691 565.

692 Guo X, Wang L, Zhang L, Li S, Hao J. Nitrogenous emissions from the catalytic pyrolysis of
693 waste rigid polyurethane foam. Journal of Analytical and Applied Pyrolysis 2014; 108:
694 143-150.

695 Guo X, Zhang W, Wang L, Hao J. Comparative study of nitrogen migration among the products
696 from catalytic pyrolysis and gasification of waste rigid polyurethane foam. Journal of
697 Analytical and Applied Pyrolysis 2016; 120: 144-153.

698 He M, Xiao B, Hu Z, Liu S, Guo X, Luo S. Syngas production from catalytic gasification of waste
699 polyethylene: Influence of temperature on gas yield and composition. International Journal
700 of Hydrogen Energy 2009; 34: 1342-1348.

701 Hilding A. Europe's bedding industry meet in Budapest. 2014;
702 http://www.hildinganders.com/good-stories/good-thinking/europes-bedding-industry-
703 met-in-budapest

704 Jansson S, Fick J, Tysklind M, Marklund S. Post-combustion formation of PCDD, PCDF, PCBz,
705 and PCPh in a laboratory-scale reactor: Influence of dibenzo-p-dioxin injection.
706 Chemosphere 2009; 76: 818-825.

707 Kaivosoja T, Virén A, Tissari J, Ruuskanen J, Tarhanen J, Sippula O, et al. Effects of a catalytic
708 converter on PCDD/F, chlorophenol and PAH emissions in residential wood combustion.
709 Chemosphere 2012; 88: 278-285.

710 Katami T, Yasuhara A, Okuda T, Shibamoto T. Formation of PCDDs, PCDFs, and Coplanar
711 PCBs from Polyvinyl Chloride during Combustion in an Incinerator. Environmental
712 Science & Technology 2002; 36: 1320-1324.

713 Kwon E, Castaldi MJ. Investigation of mechanisms of polycyclic aromatic hydrocarbons (PAHs)
714 initiated from the thermal degradation of styrene butadiene rubber (SBR) in N2
715 atmosphere. Environmental science & technology 2008; 42: 2175-2180.

716 Liu WX, Dou H, Wei ZC, Chang B, Qiu WX, Liu Y, et al. Emission characteristics of polycyclic
717 aromatic hydrocarbons from combustion of different residential coals in North China.
718 Science of The Total Environment 2009; 407: 1436-1446.

719 Lönnermark A, Blomqvist P. Emissions from an automobile fire. Chemosphere 2006; 62: 1043-
720 1056.

721 Mark HF. Encyclopedia of polymer science and technology, concise: John Wiley & Sons, 2013.

722 Market Research. Global Memory Foam Mattress Market 2015 - 2019. Market Research, 2015,
723 pp. 169.

724 Mohammed MOA, Song W-w, Ma Y-l, Liu L-y, Ma W-l, Li W-L, et al. Distribution patterns,
725 infiltration and health risk assessment of PM2.5-bound PAHs in indoor and outdoor air in
726 cold zone. Chemosphere 2016; 155: 70-85.

727 Moltó J, Egea S, Conesa JA, Font R. Thermal decomposition of electronic wastes: Mobile phone
728 case and other parts. Waste Management 2011; 31: 2546-2552.

729 Moltó J, Font R, Conesa JA. Study of the organic compounds produced in the pyrolysis and
730 combustion of used polyester fabrics. Energy & fuels 2006; 20: 1951-1958.

731 Moltó J, Font R, Gálvez A, Conesa JA. Pyrolysis and combustion of electronic wastes. Journal of
732 Analytical and Applied Pyrolysis 2009; 84: 68-78.

733 Moltó J, Font R, Gálvez A, Rey MD, Pequenín A. Analysis of dioxin-like compounds formed in
734 the combustion of tomato plant. Chemosphere 2010; 78: 121-126.

735 NATO/CCMS NATOCoCoMS. Scientific basis for the development of international toxicity
736 equivalency factor (I-TEF) method of risk assessment for the complex mixtures of dioxins
737 and related compounds. . Report No. 187. 1988.

738 Nazaré S, Davis RD, Butler K. Assessment of factors affecting fire performance of mattresses: a
739 review. Fire Science Reviews 2012; 1: 1-27.

740 Nisbet ICT, LaGoy PK. Toxic equivalency factors (TEFs) for polycyclic aromatic hydrocarbons
741 (PAHs). Regulatory Toxicology and Pharmacology 1992; 16: 290-300.

742 Paraschiv M, Kuncser R, Tazerout M, Prisecaru T. New energy value chain through pyrolysis of
743 hospital plastic waste. Applied Thermal Engineering 2015; 87: 424-433.

744 PFA. Examining Viscoelastic Flexible Polyurethane Foam. 2003; 11. 1

745 Pongpiachan S, Tipmanee D, Khumsup C, Kittikoon I, Hirunyatrakul P. Assessing risks to adults
746 and preschool children posed by PM2.5-bound polycyclic aromatic hydrocarbons (PAHs)
747 during a biomass burning episode in Northern Thailand. Science of The Total Environment
748 2015; 508: 435-444.

749 Recari J, Berrueco C, Abelló S, Montané D, Farriol X. Gasification of two solid recovered fuels
750 (SRFs) in a lab-scale fluidized bed reactor: Influence of experimental conditions on process
751 performance and release of HCl, H2S, HCN and NH3. Fuel Processing Technology 2016;
752 142: 107-114.

753 Reisen F, Bhujel M, Leonard J. Particle and volatile organic emissions from the combustion of a
754 range of building and furnishing materials using a cone calorimeter. Fire Safety Journal
755 2014; 69: 76-88.

Sánchez NE, Callejas A, Millera Á, Bilbao R, Alzueta MU. Influence of the Oxygen Presence on Polycyclic Aromatic Hydrocarbon (PAH) Formation from Acetylene Pyrolysis under Sooting Conditions. Energy & Fuels 2013; 27: 7081-7088.

Sarigiannis DA, Karakitsios SP, Zikopoulos D, Nikolaki S, Kermenidou M. Lung cancer risk from PAHs emitted from biomass combustion. Environmental Research 2015; 137: 147-156.

Schuetzle D, Schuetzle R, Kent Hoekman S, Zielinska B. The effect of oxygen on formation of syngas contaminants during the thermochemical conversion of biomass. International Journal of Energy and Environmental Engineering 2015; 6: 405-417.

Shoaib S, Shahzad Maqsood K, Nafisa G, Waqas A, Muhammad S, Tahir J. Synthesis and Characterization of Visco-Elastic (VE) Polyurethane Foam. International Journal of Innovation and Applied Studies 2014; 9: 1878-1886.

Shu Y, Zhang F, Wang H, Zhu J, Tian G, Zhang C, et al. An experimental study of NO reduction by biomass reburning and the characterization of its pyrolysis gases. Fuel 2015; 139: 321-327.

Simón D, Borreguero AM, de Lucas A, Rodríguez JF. Glycolysis of viscoelastic flexible polyurethane foam wastes. Polymer Degradation and Stability 2015; 116: 23-35.

Singh S, Prakash V. The effect of temperature on PAHs emission from incineration of acrylic waste. Environmental Monitoring and Assessment 2007; 127: 73-77.

Stec AA, Readman J, Blomqvist P, Gylestam D, Karlsson D, Wojtalewicz D, et al. Analysis of toxic effluents released from PVC carpet under different fire conditions. Chemosphere 2013; 90: 65-71.

Terakado O, Yanase H, Hirasawa M. Pyrolysis treatment of waste polyurethane foam in the presence of metallic compounds. Journal of Analytical and Applied Pyrolysis 2014; 108: 130-135.

Thomas S, Wornat MJ. The effects of oxygen on the yields of polycyclic aromatic hydrocarbons formed during the pyrolysis and fuel-rich oxidation of catechol. Fuel 2008; 87: 768-781.

Tian Y, Zhang J, Zuo W, Chen L, Cui Y, Tan T. Nitrogen Conversion in Relation to NH3 and HCN during Microwave Pyrolysis of Sewage Sludge. Environmental Science & Technology 2013; 47: 3498-3505.

US EPA. Method 1613. Tetra- through Octa-Chlorinated Dioxins and Furans by Isotope Dilution HRGC/HRMS. Test Methods for Evaluating Solid Waste Physical/Chemical Methods (SW-846). United States Environmental Protection Agency. Office of Solid Waste, Springfield: National Technical Information Service, 1994b.

US EPA. Procedure for collection and analysis of ammonia in stationary sources (CTM-027). United States Environmental Protection Agency, Washington, D.C., 1997.

US EPA. Handbook for air toxic emission inventory development. Volume I: Stationary sources. United States Environmental Protection Agency. Office of Air Quality Planning and Standards, 1998.

US EPA. Method 9056A. Determination of inorganic anions by ion chromatography. In: US EPA, editor. SW-846. United States Environmental Protection Agency, Office of Solid Waste, Washington, D.C., 2000.

US EPA. Method 3545A: Pressurized Fluid Extraction (PFE). Revision 1. Test Methods for Evaluating Solid Waste Physical/Chemical Methods (SW-846). United States Environmental Protection Agency. Office of Solid Waste, Washington, D.C., 2007, pp. 1-16.

US EPA. Method 5050. Bomb preparation method for solid waste. In: US EPA, editor. SW-846. United States Environmental Protection Agency, Office of Water, Office of Science and Technology, Spfingfield, 2007a.

US EPA. Method 1668C. Chlorinated Biphenyl Congeners in Water, Soil, Sediment, Biosolids, and Tissue by HRGC/HRM. . United States Environmental Protection Agency. Office of Water. Office of Science and Technology, Washington, D.C., 2010.

US EPA. Method 8270D. Semivolatile organic compounds by GC/MS. Test Methods for Evaluating Solid Waste Physical/Chemical Methods (SW-846). United States Environmental Protection Agency. Office of Solid Waste, Washington, D.C., 2014.

Van den Berg M, Birnbaum LS, Denison M, De Vito M, Farland W, Feeley M, et al. The 2005 World Health Organization Reevaluation of Human and Mammalian Toxic Equivalency Factors for Dioxins and Dioxin-Like Compounds. Toxicological Sciences 2006; 93: 223-241.

Watanabe M, Nakata C, Wu W, Kawamoto K, Noma Y. Characterization of semi-volatile organic compounds emitted during heating of nitrogen-containing plastics at low temperature. Chemosphere 2007; 68: 2063-2072.

Wu C, Williams PT. Effects of Gasification Temperature and Catalyst Ratio on Hydrogen Production from Catalytic Steam Pyrolysis-Gasification of Polypropylene. Energy & Fuels 2008; 22: 4125-4132.

Wu Q, Wei J. Prediction of Inter-Provincial Carbon Dioxide Emissions in China: Based on Logistic Model. 2015 International Conference on Education Reform and Modern Management. Atlantis Press, 2015.

Yang Z, Zhang S, Liu L, Li X, Chen H, Yang H, et al. Combustion behaviours of tobacco stem in a thermogravimetric analyser and a pilot-scale fluidized bed reactor. Bioresource Technology 2012; 110: 595-602.

Zhan M-X, Fu J-Y, Chen T, Lin X-Q, Li X-D, Yan J-H, et al. Suppression of dioxins by S-N inhibitors in pilot-scale experiments. Environmental Science and Pollution Research 2016: 1-15.

Zhang H-J, Ni Y-W, Chen J-P, Zhang Q. Influence of variation in the operating conditions on PCDD/F distribution in a full-scale MSW incinerator. Chemosphere 2008; 70: 721-730.

Zhang Y, Kajitani S, Ashizawa M, Miura K. Peculiarities of Rapid Pyrolysis of Biomass Covering Medium- and High-Temperature Ranges. Energy & Fuels 2006; 20: 2705-2712.

Zhou H, Wu C, Onwudili JA, Meng A, Zhang Y, Williams PT. Influence of process conditions on the formation of 2–4 ring polycyclic aromatic hydrocarbons from the pyrolysis of polyvinyl chloride. Fuel Processing Technology 2016; 144: 299-304.

Zhu C, Liu S, Liu H, Yang J, Liu X, Xu G. NOx emission characteristics of fluidized bed combustion in atmospheres rich in oxygen and water vapor for high-nitrogen fuel. Fuel 2015; 139: 346-355.

Tables

Table 1. Summary of the experiments.

Table 2. Gases and volatile compounds (ppm) detected from the pyrolysis (P) and combustion (C) of VMF at four different temperatures. The average value and standard deviation calculated from two combustion experiments at 850ºC are also shown.

Table 3. Emissions of PCDD/Fs and dl-PCBs from pyrolysis (P) and combustion (C) runs of VMF at different temperatures.

Table 4. Comparison of PCDD/F toxicity levels obtained in the combustion of different materials

Figures

Figure 1. Evolution of HCN (A), NH3 (B) and NO (C) in pyrolysis (P) and combustion (C) experiments at different temperatures.

Figure 2. Main PAHs detected in pyrolysis and combustion experiments at different temperatures.

Figure 3. Toxicity (as B[a]Pe) and total PAH yields from the pyrolysis and combustion of VMF at 550, 650, 750 and 850ºC.

Figure 4. Molecular structure of 2,4-TDI, 2,6-TDI (monomers of polyurethane foams) and o-Toluidine (semivolatile compound detected).

Figure 5. Congener profiles of chlorinated phenols during pyrolysis (P) and combustion (C) of viscoelastic memory foam (VMF) at four different temperatures (550, 650, 750 and 850ºC (average value from duplicates runs)).

Figure 6. dl-PCB congener profiles obtained in pyrolysis (P) and combustion (C) experiments at four different temperatures (550, 650, 750 and 850ºC)